

Experimental Investigation of Discrete Normal Injection for Supersonic Wing Circulation Control

Ben Halambeck*, Casey Chamberlain†, Jonathan Edwards‡, Tyler Keam§, Milan Lowe¶, Tyler Mutchnick||,
Avery Rosario**, Aditya Sivaraman††, Jack Tyree‡‡,
Virginia Polytechnic Institute and State University, Blacksburg, VA, 24060

Wing Circulation Control (WCC) is a promising technology that aims to replace the various complexities associated with conventional control surfaces. Supersonically blown air through openings on specially designed and shaped trailing edges of both the wings and tail allows for the controlled manipulation of the pressure gradient on the wing, thus allowing for aerodynamic forces to be applied - allowing for the same amount of control authority as conventional control surfaces. Due to size constraints imposed by the testing facility, however, the airfoil was unable to have compressed air blown over the trailing edge, but rather the air was blown out of a hole located on the upper surface at roughly the mid-span location. Tests were conducted at Mach numbers of 0–1 with compressed air on and off. Furthermore, the same tests were conducted from 1.5–1.75. Results showed that the blown air was most effective in the transonic region, with the greatest measurable difference between compressed air on and off being roughly 2.9 lbs. The difference in force readings was rather insignificant at high Mach numbers, but did demonstrate successful deflection in the formed shockwave, as shown in BOS imaging. We can conclude that WCC does promote the possibility of being useful in applications relevant to high maneuverability aircrafts.

I. Nomenclature

M	=	Mach number
θ	=	Shock angle (degrees)
C_L	=	Coefficient of lift
PSI	=	Pounds per square inch
AoA	=	Angle of Attack (degrees)
BOS	=	Background-Oriented Schlieren
WCC	=	Wing Circulation Control
APPL	=	Advanced Propulsion and Power Laboratory

II. Introduction

Wing Circulation Control, shortened to *WCC*, has recently emerged as a promising potential alternative solution for maneuvering flight vehicles, specifically without the use of conventional control surfaces. A significant use-case is for supersonic aircraft wherein design considerations prevent having conventional control surfaces because of mechanical complexity, a high-temperature environment, and shock interactions that reduce the reliability of flaps, rudders, and

*Undergraduate Researcher, Department of Aerospace and Ocean Engineering, benh03@vt.edu.

†Undergraduate Researcher, Department of Aerospace and Ocean Engineering, caseyc20@vt.edu

‡Undergraduate Researcher, Department of Aerospace and Ocean Engineering, jonathanedwards@vt.edu

§Undergraduate Researcher, Department of Aerospace and Ocean Engineering, tykk@vt.edu.

¶Undergraduate Researcher, Department of Aerospace and Ocean Engineering, milanlowe@vt.edu

||Undergraduate Researcher, Department of Aerospace and Ocean Engineering, tylerm26@vt.edu.

**Undergraduate Researcher, Department of Aerospace and Ocean Engineering, averynr19@vt.edu

††Undergraduate Researcher, Department of Aerospace and Ocean Engineering, asivaraman29@vt.edu.

‡‡Undergraduate Researcher, Department of Aerospace and Ocean Engineering, jackt03@vt.edu.

elevators. WCC provides fluid momentum in place of rotating parts to alter the flow behavior over control surfaces, thus providing changes in aerodynamic forces.

This study is inspired by jet-based control technologies utilized throughout the BAE Systems MAGMA UAV program, as well as utilizing the basic principles of the Coanda effect. The MAGMA system used engine bleed air routed throughout nozzles as a substitute for mechanical actuation. However, most demonstrations of the technology are still limited to subsonic regimes [1]. Using WCC in supersonic flows remains a largely unexplored area due to a myriad of associated complexities such as compressibility limitations, shock formation, and unpredictable boundary-layer behavior.

The goal of this experiment was validate whether discrete normal air injection at high Mach numbers (up to 1.75) could produce any meaningful aerodynamic effects. In particular, we sought to examine the impact of injection on lift force production and shockwave behavior using both force sensors and BOS imaging.

III. Experimental Setup

The test article was a 3D-printed symmetric airfoil with internal ducts designed to route compressed air from the shop supply into one discrete trailing edge port. The airfoil was mounted on a steel base via an aluminum bracket. This was accomplished through squeeze pins. Additional squeeze pins also ensured the airfoil remained at an angle of zero degrees. The bracket was bolted to two load cells, which were also connected to the mounting plate. In order to increase accuracy of the force readings, the mounting plate was 20 mm shorter than the load cells to allow for complete load bearing from the effects of the increased lift. This was also connected to the test stand's rail, seen in Figure 2. The wires of the leftmost load cell was connected to a HX711 load cell amplifier. This load cell amplifier was connected to an Arduino, which was connected to the laptop. These connections are shown in Figure 3, with the exception of the laptop. Two load cells were used in the experiment setup, but only one was used for collecting data. This was done as using both would have complicated both the code used by the Arduino, as well as the layout of various components, as an additional load cell amplifier would have to be used. As such, the rightmost load cell was used just for connecting to the bracket and mount.

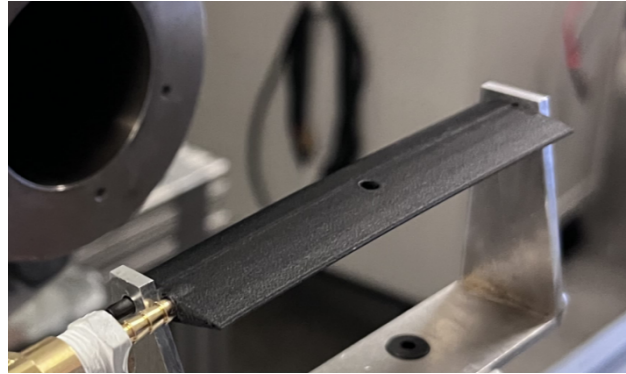


Fig. 1 Symmetrical Airfoil Used for Testing.

An eighth inch Tygon tube was fitted into the flexible airfoil inlet via a barbed connection and clamped in place at the shop air port to provide compressed air. For safety reasons within the laboratory, the pressure sensors could not be located near the test section; thus, the exit pressure PSI was estimated based on upstream pressure conditions. The entire setup would then be shifted into Virginia Tech's APPL supersonic jet rig, where a controlled Mach sweep proceeded from 0 to 1 and then from 1.5 to 1.75.

A BOS system was set up perpendicular to the nozzle exit to visualize changes in the flow field. A Flir machine vision monochromatic high speed camera was used at one end to physically capture the airfoil during tests. Opposite of it, a monitor with a background of randomly placed, small black dots served as the background of the pictures. This allowed for Particle Image Velocimetry (PIV) techniques to be used to produce BOS images. Using PIVlab in MATLAB, before and after pictures are compared, where the "before" image is when the jet rig is off. The "after" image is with the jet rig on at the desired moment in time. These two pictures are compared, where the refractions caused by the shockwaves distort the background of the monitor. To the camera, this is seen as a change in the locations of the dots. The displacement between dots in both pictures are used to make the BOS images seen in the Results and

Discussion section.

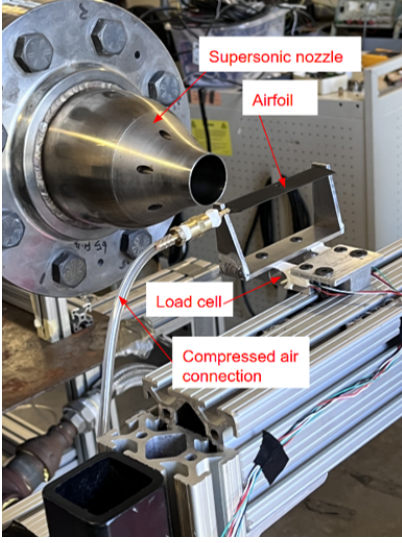


Fig. 2 Experimental setup featuring airfoil, load cell bracket, and BOS imaging configuration.

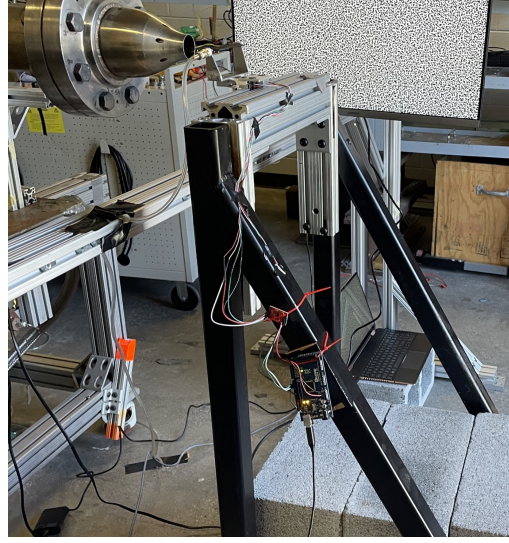


Fig. 3 Experimental setup (test stand).

IV. Test Procedure

Each run in the supersonic tunnel began with baseline data acquisition with the air injection off. After baseline data collection, compressed air runs were done by manually using a control button on the Matlab GUI interface to control the compressed air. Force data was recorded continuously on a laptop through a custom Arduino serial interface. Each Mach number setting was held long enough to establish time-averaged data with visible minimum and maximum ranges.

For BOS imaging, photographs were taken using the Mach sweep of 0-1 with and without compressed air. This was also completed at Mach numbers of 1.5, 1.65, and 1.75 with the APPL jet rig being equipped with the supersonic nozzle. During the test, images were taken using the high speed camera, with the monitor serving as the background of the pictures. These images were processed using optical flow algorithms to quantify angular shifts in the shock location. Calibration images of a known grid spacing were taken to convert pixel deflections into physical angles.

Due to limited tunnel time and rigid scheduling, a single airfoil was used throughout the experiment. Although this added some wear-related uncertainty, it allowed for a consistent basis of comparison between runs. The airfoil was monitored during testing for flutter and deformation to ensure accuracy of the data.

V. Results and Discussion

A. Force Data

Force measurements were averaged with respect to time for each Mach number region. Figure 2 shows the data averaged over time at various Mach regions from 0 to 1. The dots represent the average force value during the sweep, while the error bars show the highest and lowest readings in the sweep. The red data points are where the compressed air is on, and the blue data point is when the compressed air is off.

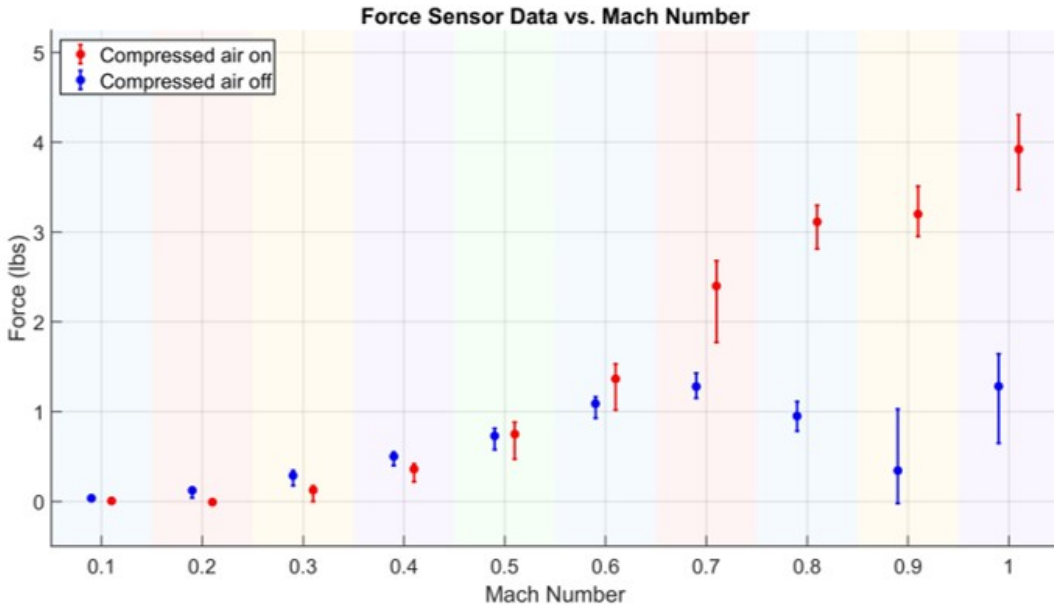


Fig. 4 Bar graph showing average force on the airfoil with and without compressed air across different Mach numbers.

The most significant force increase occurred between Mach 0.6 and Mach 1. There was also a slight zero to negative impact of the compressed air at low Mach numbers. A trend that was discovered was that the error bars increased at higher Mach regions. This is most likely due to undesired vibrations that ultimately impacted the data.

Since a symmetric airfoil was used, it was intended that the force readings would be zero. However, the force sensor was sensitive to changes in normal force produced by the jet. Another possible source of error is that the airfoil may not have been aligned perfectly with the stream. Even off by a fraction of a degree can make a difference in the force readings.

Due to the non-zero compressed air measurements, a separate normalized plot was created to better visualize the data. Figure 3 features data that were taken during the same Mach sweep test as Figure 2, with the addition of the supersonic Mach numbers.

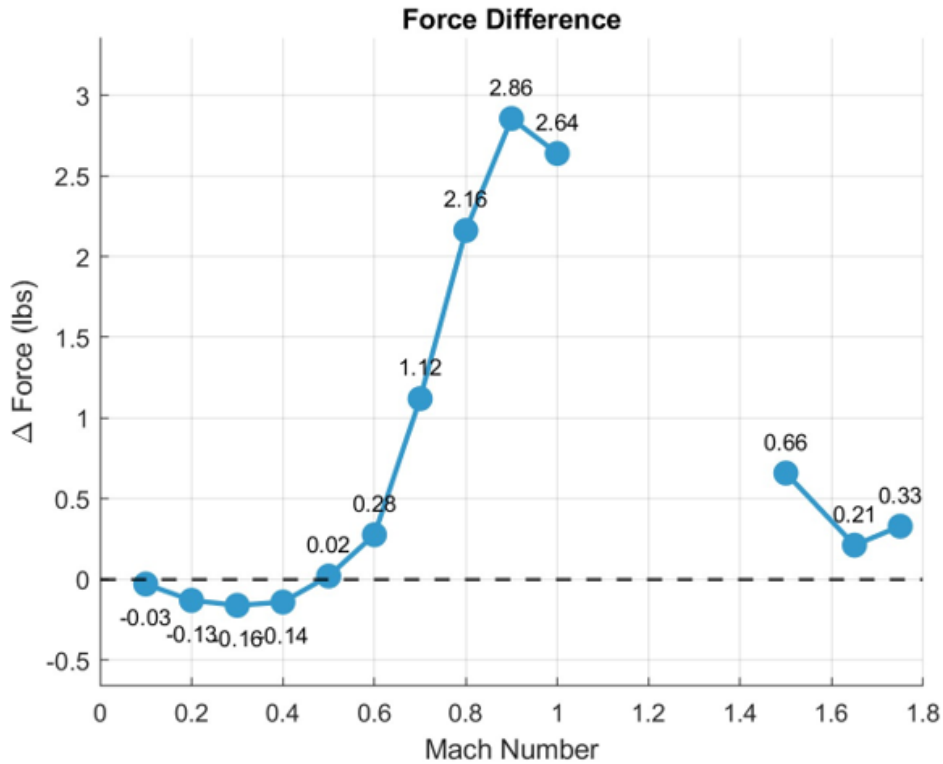


Fig. 5 Force difference between compressed air on and off, normalized across Mach range. Peak performance observed in the transonic regime.

It is evident that there are diminishing returns on the impact of the compressed air at supersonic speeds. The impact of the compressed air was most effective in the transonic region. It is important to note that there was slight deformation of the airfoil at Mach 1.75, and may have impacted the other supersonic results.

B. BOS Imaging and Shock Deflection

BOS outputs show the velocity field, on and around the airfoil, of the flow exiting the nozzle. At Mach 1.65, the shock expansion waves are located aft of the airfoil and deflected up about 13° with no compressed air injection. But with compressed air injection of 150 PSI, the shock angle is about 19° . Indicating that the difference in angles is roughly 6° . Demonstrating that the local supersonic flow was altered by the air injection, it was confirmed that it has the ability to adjust the pressure distribution over the airfoil.

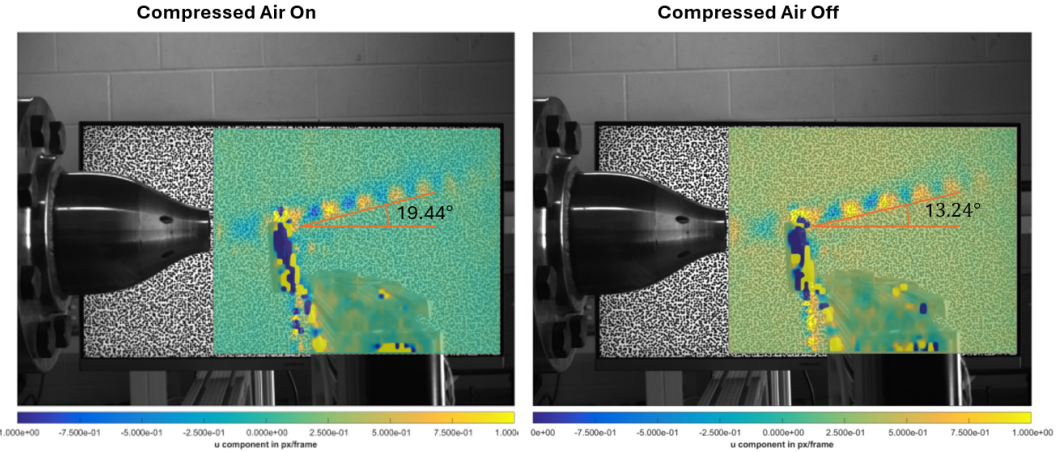


Fig. 6 Side-by-side BOS image comparison at Mach 1.65 with compressed air off (left) and on (right). The shock location visibly shifts forward with injection.

To better illustrate this shock angle change, we created a schematic diagram overlaying both the compressed air on and off cases. The angle delta was measured to be approximately 6.2° , supporting our BOS image results.

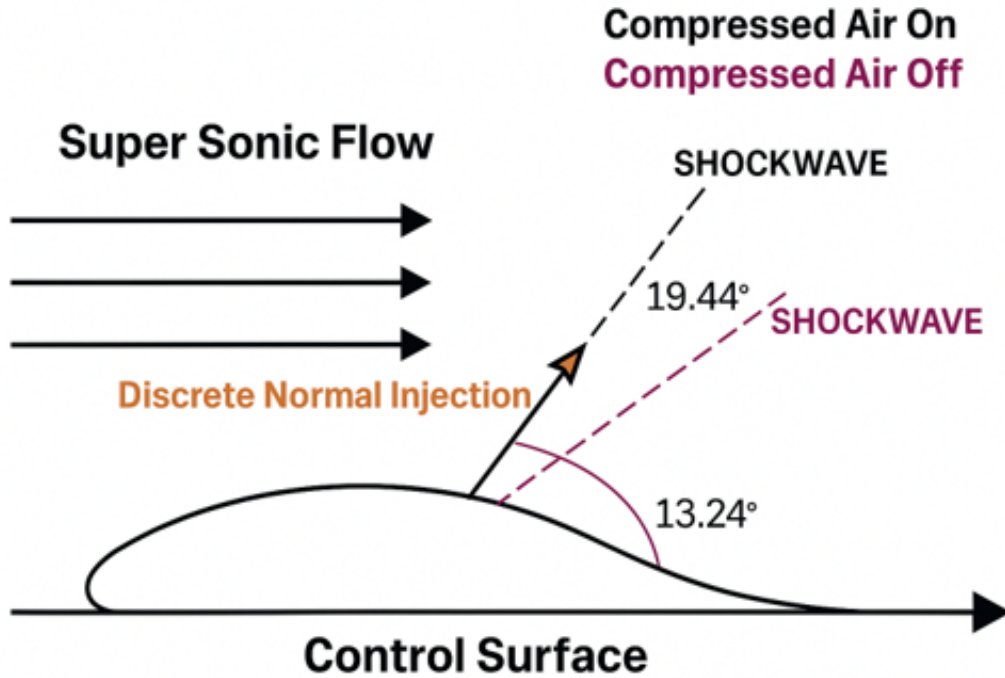


Fig. 7 Shockwave angle diagram showing Mach deflection change of 6.2° between compressed air on (13.24°) and off (19.44°). BOS imaging confirmed the angular shift.

C. Tradeoffs and Limitations

Testing revealed both the strengths and weaknesses of the normal air injection. The highest performing region for the compressed air was in the transonic region. This is applicable to a fighter aircraft as many combat turns occur in the transonic region. As modern global militaries are focusing on developing fighters with remote control capabilities, input lag is becoming a prevalent issue. Therefore, being able to increase forces and induce aerodynamic moments relatively instantaneously helps close the gap in control.

From the BOS imaging, it is evident that the compressed air influences the Mach deflection angle which provides a source of control authority at high Machs. Even with the small supersonic force readings, an aircraft will still have positive control at supersonic speeds due to its ability to generate specific aerodynamic moments from the deflections that the compressed air produces.

Even small aerodynamic forces can make a major impact on a fighters performance at high Mach numbers. At high speeds, a fighter aircraft needs to be able to track targets which is sufficiently completed with minor force adjustments. Injected compressed air can make these small adjustments faster than traditional control surfaces..

While there are many positive impacts from the data, it is important to recognize that testing also showed limitations of compressed air injection. One clear one is that there are diminishing returns at higher Mach Numbers. This may have been influenced by possible deformation in the airfoil, due to limitations in compressed air. All tests were ran at 150 psi, and it is possible that a higher pressure is necessary to produce a significant force difference.

There was also poor performance at low subsonic Mach numbers. This is detrimental to takeoff and landing performance as there was no evidence of control authority at low speeds. Additionally, the change in Mach deflection angle may induce pressure drag that can generate worse turning performance.

There were several other limitations faced by the experiment, which have impacted the quality and extent of the results. The small test section imposed tight constraints on the flow through it and was inadequate to gather aerodynamics data that would be truly representative.

The airfoil was constructed in plastic using 3D printing, so irregularities in surface roughness and geometric inaccuracies could possibly have affected its performance. We never got to measure the exact pressure drop across the section, thus leaving our pressure distribution analysis with a missing piece. The control room was packed, making it difficult to work around all the equipment; therefore, it stopped us from fine-tuning the controls in real time very accurately.

In addition, the restrictions on funding further set a constraint on the amount of time we could spend at the laboratory, in turn limiting not only the number of trials we could run but also the repeatability of the results. Finally, whereas we closely followed an existing standard design for an airfoil shape, It cannot be discounted that slight variations occurring during manufacture would have diverged some airfoil performance outcomes from theoretical expectations of ideal performance.

VI. Future Revisions and Design Improvements

To further enhance this research several targeted improvements were devised that will increase accuracy, consistency, and overall system performance. The listed recommended modifications are as follows:

- **Metal Airfoil Construction:** Replace the plastic airfoil with a metal airfoil to eliminate deformation effects at greater span of flow regimes. This will allow greater investigation into different Mach regions.
- **Integrated Pressure Taps:** Add pressure sensors at injection exit. along the airfoil to quantify flow response and PSI effects more precisely.
- **Trailing Edge Coandă Surface:** Incorporate a rounded trailing edge geometry to take advantage of the Coandă effect.
- **Variable PSI Control System:** Install a remote controlled pressure regulation unit for variable pressure injection. This will enable more nuanced testing of the exit pressures effect on boundary layer interactions.
- **Mach 1–1.5 Testing Focus:** Since the best results for our symmetric airfoil occurred close to Mach 1, the testing region should be increased between Mach 1–1.5 to closely mimic the entire combat regime for fighter aircraft.

The upgrades listed above will enable a more comprehensive evaluation of discrete normal injection's viability as a practical high speed flow control method.

VII. Conclusion

Discrete normal air injection shows promising results regarding achieving solid-state control in a supersonic aircraft. The experiment demonstrated measurable aerodynamic changes, primarily in the transonic regime, as well as in the validation of the force data and the concept with BOS imaging. The limitations of the system included working with a fixed PSI and a plastic construction. Regardless, shock deflection was visible, and lift was increased - these results warrant further exploration into the concept, however using a more refined design.

VIII. References

IX. References

- [1] A. Kay, Successful first flight trial completion of unmanned aerial vehicle, magma., <https://www.baesystems.com/en/article/first-magma-flight-trials> (accessed Apr. 24, 2025).
- [2] C. Chamberlain et al., “4/8/25 Virginia Tech Team 7 Senior Design Experiment,” YouTube, https://www.youtube.com/playlist?list=PLeAvOwo730jbIsqLFFt2z7mh_LGpEspNe (accessed May 8, 2025).

Acknowledgments

The members of Team 7 *Lucky 7* would like to graciously thank Dr. Davoudi, Sanjay Balasubramaniam, Dr. Lowe, Mr. Monk, Mr. Doby, and Matthew Morrison, for their continued guidance and support throughout the duration of the Senior Design Project, as well as access to the APPL Lab and other project-critical materials. Finally, we would like to thank the Department of Aerospace and Ocean Engineering at Virginia Tech, for the exceptional educational support and the outstanding academic program it has provided over the course of our time here.